Journal of Nano- and Electronic Physics
Vol. **18** No 1, 01032(6pp) (2026)

Журнал нано- та електронної фізики
Том **18** № 1, 01032(6cc) (2026)

OPEN ACCESS

REGULAR ARTICLE

Effect of Current Density on the Chemical Composition of ZnS Nanoparticles in the Absence and Presence of the ATLAS FLUKA Surfactant

O.V. Smitiukh[1,*], O.M. Yanchuk[2], M.O. Pukh[2], V.M. Kordan[3], O.V. Marchuk[1]

[1] *Lesya Ukrainka Volyn National University, 43025 Lutsk, Ukraine*
[2] *Novovolynsk Scientific Lyceum, 45400 Novovolynsk, Ukraine*
[3] *Ivan Franko National University of Lviv, 79000 Lviv, Ukraine*

(Received 13 January 2026; revised manuscript received 23 February 2026; published online 25 February 2026)

In the present study, the role of electrolysis current density in the range of 0.1-0.5 A/cm² on the formation of the phase composition, crystal lattice, particle thickness, and morphology of the powdery product obtained during the electrochemical dissolution of zinc using a carbon cathode was analyzed for the first time. The synthesis was carried out at a temperature of 90 °C and a process duration of 20 min in an inert electrolyte medium consisting of a 1 M sodium chloride solution with the addition of 0.2 M thioacetamide as a sulfur source, both in the absence and in the presence of the ATLAS surfactant. The results of X-ray phase analysis, X-ray structural analysis, and energy-dispersive X-ray analysis showed that the synthesized precipitates consist predominantly of zinc sulfide in the sphalerite modification (*α*-ZnS), with a minor amount of elemental sulfur detected. It was established that the unit cell parameters change with current density in a nonlinear manner. At the same time, the adding of ATLAS surfactant into the electrolyte during the synthesis stage leads to a noticeable decrease in the crystal lattice parameters of the final product. The thickness of zinc sulfide particles, estimated using the Scherrer formula, exhibits a tendency to increase with increasing current density, ranging from approximately 4 to 5 nm. The addition of ATLAS surfactant to the electrolyte has little effect on the particle thickness. Analysis of SEM images of samples MP5 and MP10, synthesized at the same current density of 0.50 A/cm² but without surfactant and with 0.5 g/L ATLAS in the electrolyte, respectively, revealed a significant difference in particle sizes. The particles in sample MP10 are several times smaller than those in sample MP5, indicating the effective role of ATLAS as a particle growth stabilizer and its ability to promote the formation of a more monodisperse powder.

Keywords: Electrochemical synthesis, Nanoparticles, Zinc sulfide, Crystallographic projection.

DOI: 10.21272/jnep.18(1).01032 PACS numbers: 61.46.Df, 82.45.Aa

1. INTRODUCTION

A distinct place among nanomaterials is occupied by chalcogenides of elements from the zinc subgroup, which exhibit semiconducting properties. In particular, zinc oxide and zinc sulfide possess a wide band gap, which promotes their application in materials science. Another important aspect of research in the field of nanochemistry and nanotechnology is the search for methods and approaches to obtain particles with the narrowest possible size distribution. For this purpose, various particle growth stabilizers are employed [1-5].

Semiconductor nanomaterials are of particular interest due to their size-dependent optical, electrical, and surface characteristics, which enable their application in optoelectronics, sensing, catalysis, and energy-related technologies [6]. Significantly, chalcogenides of group II elements represent an important class of compounds owing to their chemical stability and pronounced quantum size effects.

Zinc sulfide (ZnS) is a wide-band-gap II-VI semiconductor that has been extensively investigated at the nanoscale because of its favorable electronic structure, high exciton binding energy, and environmental compatibility [7-8]. When the particle size is reduced to the nanometer scale, the properties of ZnS become strongly dependent on synthesis conditions, including particle size, crystallinity, defect density, and chemical composition [9]. Consequently, the controlled preparation of ZnS nanoparticles with narrow size distributions and well-defined composition remains a central challenge in nanochemical synthesis.

Taking into consideration of mentioned above, current density plays a key role, as it directly determines the rate of electrochemical processes and the local concentration of reactive species in the vicinity of the electrode surface. Changes in current density can lead to significant variations in particle size, morphology, defect concentration, and stoichiometry of the synthesized nanomaterials [10]. Despite numerous studies on the electrochemical synthesis of ZnS nanoparticles, the effect of current density on their chemical composition has not been sufficiently clarified, particularly in systems employing sulfur-containing precursors such as thioacetamide.

In this work, the effect of current density on the chemical composition of ZnS nanoparticles synthesized by

* Correspondence e-mail: Smitiukh.Oleksandr@vnu.edu.ua

Cite this article as: O.V. Smitiukh et al., *J. Nano- Electron. Phys.* 18 No 1, 01032 (2026) https://doi.org/10.21272/jnep.18(1).01032

electrolysis of an aqueous sodium chloride solution is investigated using a soluble zinc anode, with thioacetamide serving as a sulfur-containing precursor. The synthesis is carried out both in the absence and in the presence of ATLAS FLUKA surfactant to evaluate its role in stabilizing nanoparticle growth and modifying the chemical composition of the product. The results of this study provide insight into the nanochemical mechanisms governing ZnS nanoparticle formation and contribute to the development of controlled electrochemical synthesis strategies for semiconductor nanomaterials.

2. EXPERIMENTAL DETAILS

Nanosized precipitates were obtained by electrolysis of an aqueous solution containing NaCl and TAA, without the addition of surfactant (the first five experiments) and with the addition of ATLAS surfactant (the subsequent five experiments). Electrolysis was carried out in a galvanostatic mode at a constant temperature of 90 °C using a two-electrode system consisting of a zinc plate (anode) and a carbon rod with a surface area of 5 cm^2 (cathode), with an electrolysis duration of 20 min.

For the experiments, 1 L of electrolyte was prepared as a sodium chloride solution with a concentration of 1 M and 0.2 M TAA, and 1 L of an identical solution (1 M NaCl and 0.2 M TAA) containing 0.5 g of ATLAS surfactant. Approximately 200 mL of electrolyte was used for each experiment. In total, 10 experiments were conducted. The experiments differed in current intensity I, current density j, and applied voltage U.

The numbering of samples, the content of surfactants, and the voltage during electrolysis are presented in Table 1.

Table 1 – The numbering of samples, the content of surfactants, and the voltage during electrolysis

No	Content of surfactant, g/l	I, A	J, A/sm^2	U, V
MP1	0	0.48	0.096	1.6
MP2	0	1.00	0.200	2.4
MP3	0	1.54	0.308	3.5
MP4	0	2.00	0.400	4.1
MP5	0	2.51	0.502	4.9
MP6	0.5	0.48	0.096	1.5
MP7	0.5	1.00	0.200	2.3
MP8	0.5	1.54	0.308	3.2
MP9	0.5	2.00	0.400	4.0
MP10	0.5	2.51	0.502	4.8

The extraction of synthesized nanopowders and the mechanism of electrolytic formation of zinc sulfide are described in [11].

The powdery precipitates were analyzed by X-ray phase and structural analysis to determine their crystal structure and particle size. The chemical composition of the powders was examined using energy-dispersive X-ray microanalysis (EDX).

Particle morphology and approximate particle sizes were evaluated from images obtained using a Tescan Vega3 LMU scanning electron microscope at the Center for Collective Use of Scientific Equipment "Laboratory of Materials Science of Intermetallic Compounds" at Ivan Franko National University of Lviv. A detailed description of the microscope and the energy-dispersive microanalyzer is provided in Appendix A. X-ray diffraction patterns of the synthesized powders were recorded by the head of the X-ray laboratory using a DRON 4-13 diffractometer with Cu Kα radiation.

The results of phase analysis, carried out with using program package WINCSD of ZnS (SG *F-43m*), are presented in Fig. 1.

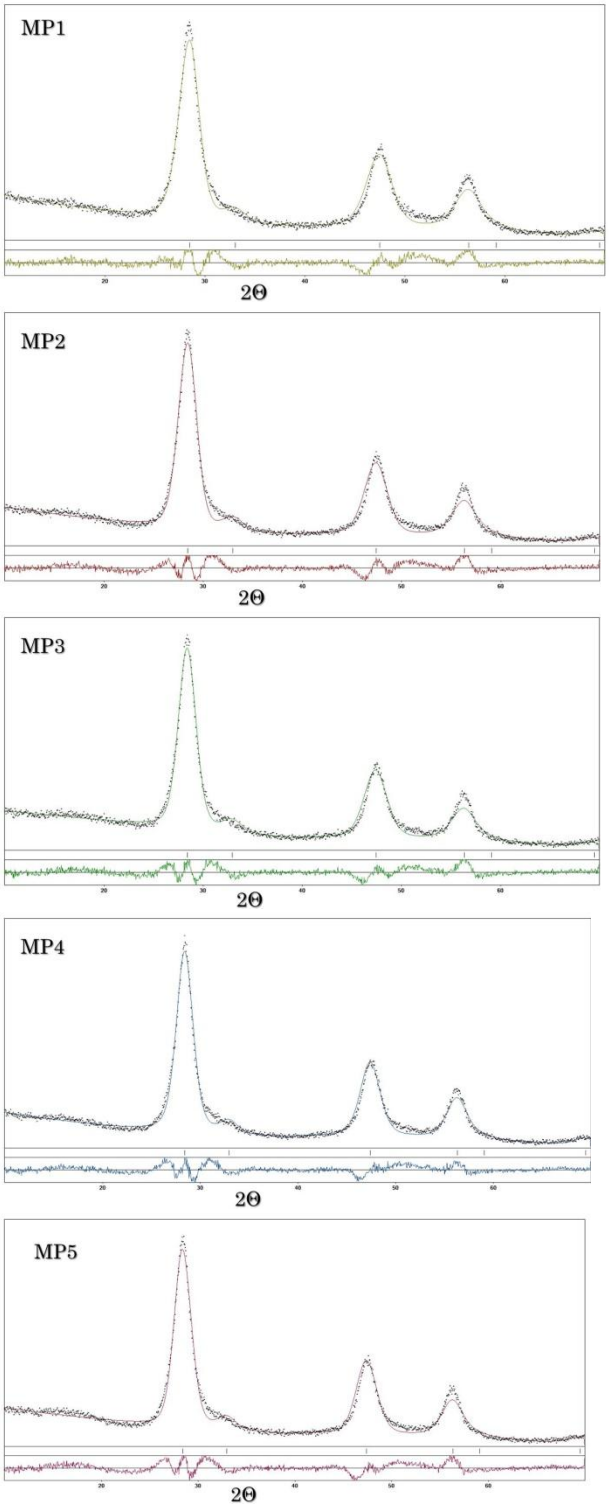

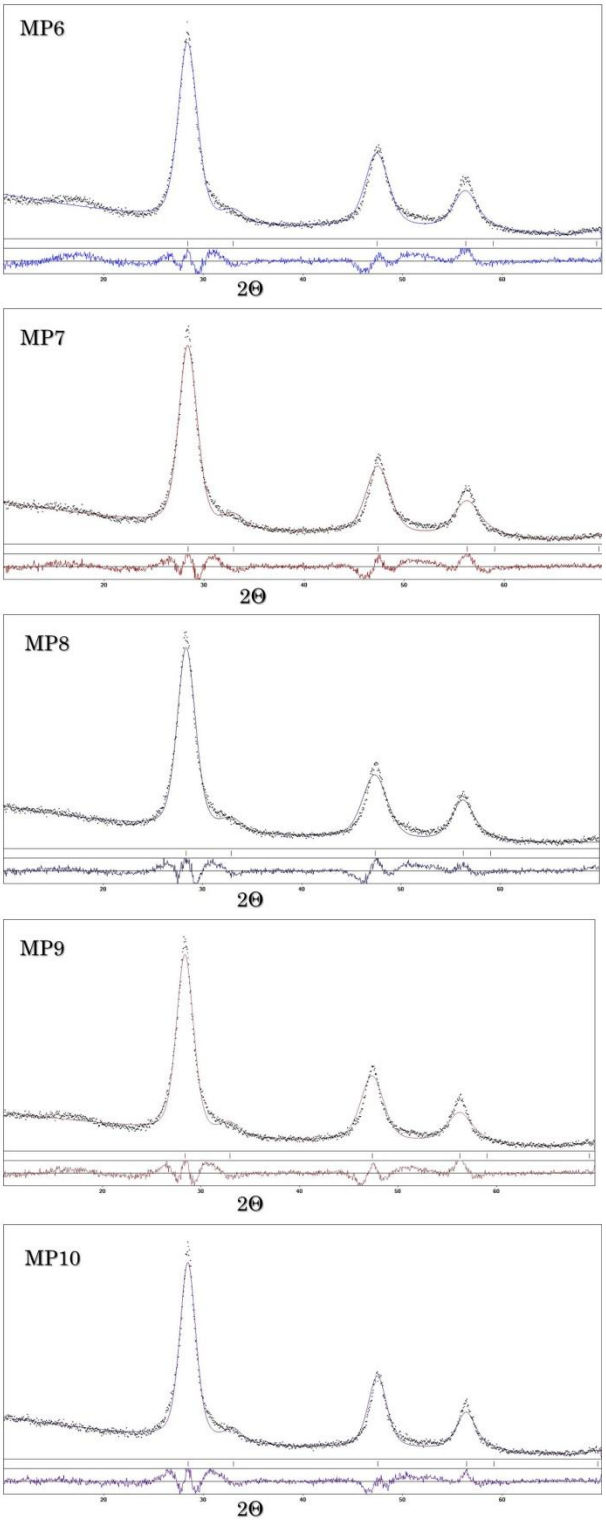

Fig. 1 – The calculated diffractograms of the samples MP1-MP5 (without ATLAS) and MP6-MP10 (in the presence of ATLAS)

The structure of α-ZnS is a cubic close-packed lattice (Fig. 2). In this structure, zinc and sulfur atoms occupy the same positions as in the diamond structure: the lattice can be described as two equivalent face-centered cubic (FCC) sublattices, each containing four atomic positions. These sublattices are displaced relative to each other by a vector in the [1/4 1/4 1/4] direction. If the lowest layer is denoted as A, the ABC stacking sequence is observed in the cubic sphalerite structure.

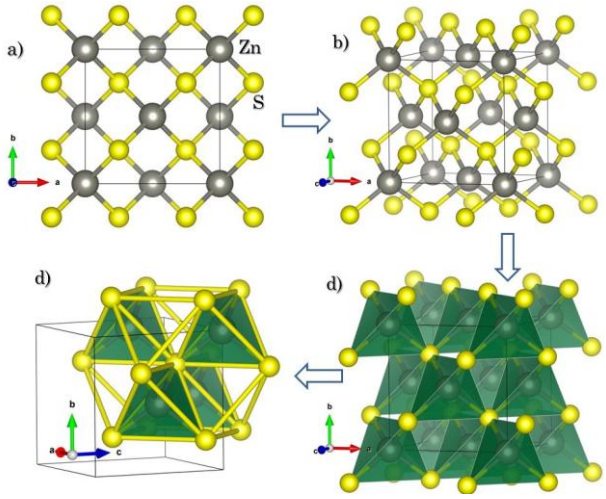

Fig. 2 – Projection of the crystalline structure of synthesized ZnS nanoparticles: a) and b) the unit cell; c) Packaging of tetrahedrons of $[ZnS_4]^{6-}$; d) second coordination environment

The results obtained using an energy-dispersive X-ray microanalyzer (EDXR analysis) are presented in Table 2.

Table 2 – The results of EDXR analysis

No	**MP1**	**MP3**	**MP5**
***j*, A/cm²**	0.096	0.308	0.502
[Atlas], g/L	0	0	0
$\chi_{\Sigma Zn}$ (mol. %)	47.89	48.74	45.85
$\chi_{\Sigma S}$ (mol. %)	52.11	51.26	54.15
χ_{ZnS} (mol. %)	95.78	97.48	91.7
χ_S (mol. %)	4.22	2.52	8.3
with ATLAS			
No	**MP6**	**MP8**	**MP10**
***j*, A/cm²**	0.096	0.308	0.502
[Atlas], g/L	0.5	0.5	0.5
$\chi_{\Sigma Zn}$ (mol. %)	45.31	48.83	48.01
$\chi_{\Sigma S}$ (mol. %)	54.69	51.17	51.99
χ_{ZnS} (mol. %)	90.62	97.66	96.02
χ_S (mol. %)	9.38	2.34	3.98

As shown by the EDX analysis results, the main product of the synthesis is zinc sulfide with sulfur impurities ranging from 2 to 9 %. Sulfur is likely formed during the electrolysis process from sulfide ions generated both as a result of electrochemical reactions and through the hydrolysis of TAA. A portion of the sulfide ions that do not have sufficient time to convert into zinc sulfide precipitate in the form of elemental sulfur.

The results of crystallographic calculations are summarized in Table 3.

All unit cell parameters are noticeably smaller for the samples obtained in the presence of a surfactant in the electrolyte. Regarding the effect of current density, a stepwise, nonlinear dependence is observed (Fig. 3-5).

Table 3 – The results of crystallographic calculations of the samples MP1-MP10

No	*a*, Å	*V*, Å³	*d*(Zn-S), Å	*j*, A/cm²	[Atlas], g/L
MP1	5.399	157.4	2.338	0.096	0
MP2	5.401	157.6	2.339	0.200	0
MP3	5.396	157.1	2.3364	0.308	0
MP4	5.402	157.6	2.339	0.400	0
MP5	5.393	156.9	2.3353	0.502	0
MP6	5.397	157.2	2.337	0.096	0.5
MP7	5.395	157	2.3361	0.200	0.5
MP8	5.398	157.3	2.3375	0.308	0.5
MP9	5.397	157.2	2.337	0.400	0.5
MP10	5.39	156.6	2.3341	0.502	0.5

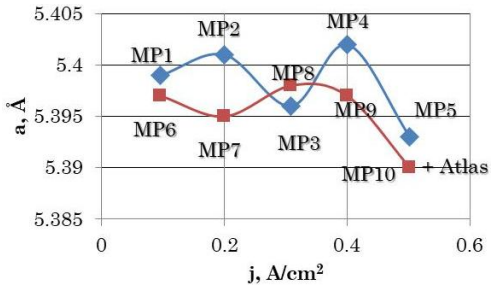

Fig. 3 – Dependence of parameter *a* of the ZnS unit cell on current density

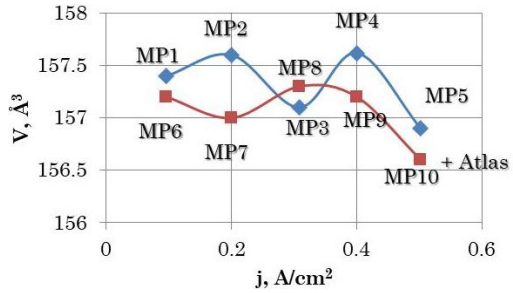

Fig. 4 – Dependence of volume (*V*) of the ZnS unit cell on current density

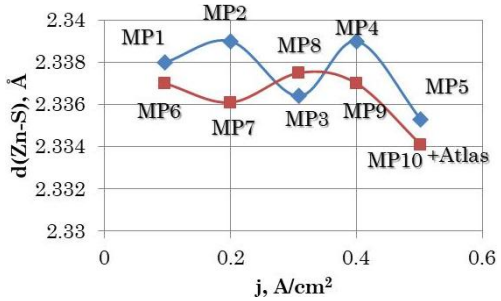

Fig. 5 – Dependence of interatomic distance Zn-S on current density

The lattice parameter *a* and the unit cell volume *V* are correlated: local maximum of a correspond to local maximum of *V*, and minimum correspond to minimum. This behavior is expected for a cubic unit cell (*V*, Å³).

The absolute variations of a (~ 0.02 Å) are small (~ 0.37 % of the average value), but statistically significant for *X*-ray diffraction measurements, as they correspond to noticeable changes in interatomic distances. A change in *V* of approximately 1 Å³ (~ 0.64 %) is also physically meaningful, since even small concentrations of interstitial defects, vacancies, or impurities can produce such shifts.

Vacancies of Zn or S, as well as interstitial Zn defects (Zn□$_i$), alter the average lattice spacing. An excess of Zn leads to an increase in *a* and *V*, whereas sulfur deficiency or compensated non-stoichiometry results in a decrease in unit cell volume due to a more compact atomic arrangement. Foreign impurities (e.g., oxygen) substituting for sulfur in the lattice may either decrease or increase the lattice parameters, depending on the substituting atom and its ionic radius. Smaller crystallites (nanoscale crystallite size *D*) often exhibit lattice expansion due to surface pressure or strain effects, whereas larger grains tend to show lattice parameters closer to literature values.

Although ZnS is the dominant phase in the overall Rietveld refinement, weak impurity phases (such as ZnO, polytypic modifications, or non-stoichiometric complexes) may affect the positions of the main diffraction peaks through peak overlap or background shifts. Local maximum (MP2, MP4) may correspond to synthesis conditions that yield the most "pure" and least defective cubic lattice, and thus larger values of *a*.

The synthesis temperature and heat-treatment duration determine the defect equilibrium: higher temperatures generally promote defect relaxation and bring the unit cell dimensions closer to their thermodynamic equilibrium values, whereas rapid cooling can "freeze in" metastable defects. MP2 and MP4 (local maxima of *a* and *V*) most likely correspond to synthesis conditions (optimal temperature, duration, and sulfur excess) that minimize vacancy concentration, resulting in the largest unit cell volume. MP5 and MP10 (minimum) are likely associated with more pronounced non-stoichiometry and possibly impurity incorporation, leading to reduce *a*. MP3 and MP6-MP9 (intermediate values) reflect a combination of partial recrystallization, partial defect relaxation, and moderate non-stoichiometry.

The particle thickness of the zinc sulfide powders was estimated using the Scherrer formula, and their morphology was also taken into account based on SEM images. As shown in Table X and Fig. 3-6, the average particle thickness decreases with increasing TAA concentration, ranging from 4 to 5 nm. Thus, it can be concluded that the zinc sulfide particles are nanosized in terms of thickness. The results also indicate a tendency for a slight increase in particle thickness with increasing current density.

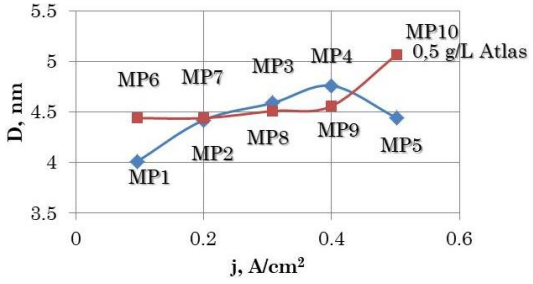

Fig. 6 – Dependence of the thickness of ZnS nanoparticles on current density

Table 4 – The results of the calculation of the thickness of the samples MP1-MP10

No	$2\theta_1$-$2\theta_2$ °	[Atlas], g/L	j, A/cm²	D, nm
MP1	2.14	0	0.096	4.01
MP2	1.94	0	0.200	4.42
MP3	1.87	0	0.308	4.59
MP4	1.8	0	0.400	4.76
MP5	1.93	0	0.502	4.44
MP6	1.93	0.5	0.096	4.44
MP7	1.93	0.5	0.200	4.44
MP8	1.9	0.5	0.308	4.51
MP9	1.88	0.5	0.400	4.56
MP10	1.69	0.5	0.502	5.07

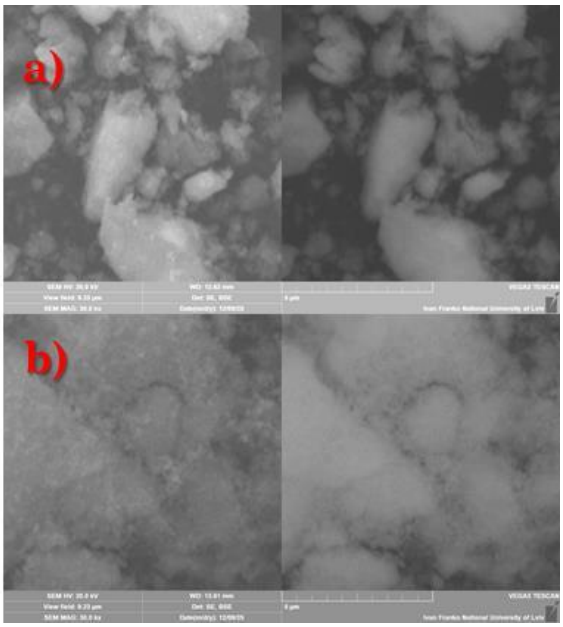

Fig. 7 – SEM photographs of samples MP5 (a) and MP10 (b), obtained at the same current density of 0.5 A/cm². Sample MP10 was synthesized with a content of 0.5 g/L of ATLAS surfactant, and sample MP5 was synthesized without surfactant

Adding ATLAS surfactant to the electrolyte does not contribute to obtaining smaller particles in thickness, in contrast to the results regarding the synthesis of cadmium sulfide and zinc oxide particles [12-14], where the surfactant significantly reduces the size.

SEM-images of the samples (for illustration, other are similar) MP5 and MP10 are presented in Fig. 7.

The question of particle morphology as well as particle width and length remains open due to the insufficient resolution of the SEM images. However, it can be stated that the zinc sulfide particles are likely to have a rounded shape with sizes below 100 nm, particularly in the case of sample MP10. Sample MP5 contains large agglomerates and coarse particles, whereas sample MP10 consists of significantly finer particles, indicating that ATLAS acts as a particle growth stabilizer and promotes the formation of a more monodisperse powder. All other samples are also composed predominantly of large agglomerates.

3. CONCLUSIONS

X-ray phase and structural analysis combined with EDX analysis revealed that the powdery precipitates synthesized by electrolysis of an aqueous sodium chloride and TAA solution using a soluble zinc anode consist of particles of the sphalerite modification of zinc sulfide (α-ZnS) along with a small fraction of elemental sulfur. Fluctuations in the crystal lattice parameters are observed as a result of variations in current density, while a reduction in these parameters is noted in the presence of ATLAS surfactant in the electrolyte during synthesis.

The thickness of zinc sulfide particles, calculated using the Scherrer method, shows a tendency to increase with increasing current density and exhibits only a weak dependence on the addition of the surfactant. The presence of ATLAS in the electrolyte at a concentration of 0.5 g/L does not lead to a reduction in ZnS particle thickness. Under the influence of current density in the range of 0.1 to 0.5 A/cm², the thickness of zinc sulfide particles varies from 4 to 5 nm.

A comparison of SEM images for samples MP5 and MP10, obtained at the same current density of 0.50 A/cm² but synthesized without surfactant and with 0.5 g/L of ATLAS in the electrolyte, respectively, demonstrates that the particle sizes in sample MP10 are several times smaller than those in sample MP5. This indicates that ATLAS acts as a particle growth stabilizer and promotes the formation of a monodisperse powder.

REFERENCES

1. A. Chatterjee, G.K. Kumar, G. Roymahapatra, H.S. Das, G. Jaishree, T.S. Rao, *Front. Nanotechnol.* **6**, 1433591 (2024).
2. M.H.K. Al-Memoori, H.A. Majeed, A. Al-Nafiey, *JUBPAS* **32** No 4, 102 (2024).
3. Z.L. Wang, *J. Phys.: Condens. Matter.* **16** No 25, R829 (2004).
4. L. Vittaya, C. Chalad, U. Sirimahachai, *ChemistrySelect* **9** No 6, e202304671 (2024).
5. X. Zhou, Z. Hayat, D.D. Zhang, M.Y. Li, S. Hu, Q. Wu, Y.F. Cao, Y. Yuan, *Processes* **11** No 4, 1193 (2023).
6. A. Belyaev, Z. Maksimenko, S. Golovynskyi, V. Kravchenko, P. Smertenko, *Semicond. Phys. Quantum Electron. Optoelectron.* **28** No 1, 004 (2025).
7. A. Tiwari, S. Bishnoi, S. Dhoble, *J. Molec. Struct.* **1349**, 143750 (2026).
8. O. Ejeromedoghene, K.O. Abdulwahab, I.A. Udofia, M. Kumi, A.O. Nejo, *Energy Adv.* **3** No 6, 1196 (2024).
9. S.I. Sadovnikov, A.V. Ishchenko, I. Weinstein, *J. Alloy. Compd.* **831**, 154846 (2020).
10. R.K. Mishra, K. Verma, D.S. Singh, *Smart Mater. Manufact.* **2**, 100052 (2023).
11. O. Yanchuk, L. Tsurkova, O. Marchuk, I. Urubkov, M. Kolcun, K. Rusek, A. El Nagga, A. Albassam, *Mater. Lett.* **169**, 131 (2016).
12. O.M. Yanchuk, O.V. Marchuk, I.A. Moroz, O.A. Vyshnevskyi, A.M. El-Naggar, A.A. Albassam, I.V. Kityk, P. Czaja, *J. Mater. Sci.: Mater. Electron.* **30** No 19, 17741 (2019).
13. R. Korol, O. Yanchuk, O. Marchuk, V. Orlov, I. Moroz, O. Vyshnevskyi, *Phys. Chem. Solid State* **22** No 2, 380 (2021).
14. O.M. Smitiukh, O.V. Marchuk, O.M. Yanchuk, Yu.O. Khmaruk, *J. Nano- Electron. Phys.* **16** No 1, 01024 (2024).

Вплив густини струму на хімічний склад наночастинок ZnS за відсутності та присутності ПАР ATLAS FLUKA

О.В. Смітюх[1], О.М. Янчук[2], М.О. Пух[2], В.М. Кордан[3], О.В. Марчук[1]

[1] *Волинський національний університет імені Лесі Українки, 43025 Луцьк, Україна*
[2] *Нововолинський науковий ліцей, 45400 Нововолинськ, Україна*
[3] *Львівський національний університет імені Івана Франка, 79000 Львів, Україна*

У даному дослідженні вперше проаналізовано роль густини струму електролізу в діапазоні 0,1-0,5 А/см^2 на формування фазового складу, кристалічної ґратки, товщини та морфології частинок порошкоподібного продукту, отриманого під час електрохімічного розчинення цинку з використанням вугільного катода. Синтез здійснювали за температури 90 °C та тривалості процесу 20 хв у середовищі індиферентного електроліту – 1 М розчину натрій хлориду з додаванням 0,2 М тіоацетаміду як джерела сульфуру, як за відсутності, так і за наявності поверхнево-активної речовини ATLAS. Результати рентґенофазового, рентґеноструктурного та енергодисперсійного рентгенівського аналізу показали, що синтезовані осади складаються переважно з цинк сульфіду у сфалеритній модифікації (α-ZnS), при цьому фіксується незначна домішка елементарної сірки. Встановлено, що параметри елементарної комірки змінюються з густиною струму за нелінійним законом. Водночас введення ПАР ATLAS до електроліту на етапі синтезу призводить до помітного зменшення параметрів кристалічної ґратки у кінцевому продукті. Оцінка товщини частинок цинк сульфіду, виконана за формулою Шеррера, засвідчила тенденцію до її зростання зі збільшенням густини струму – від приблизно 4 до 5 нм. При цьому додавання ПАР ATLAS до електроліту практично не впливає на величину товщини частинок. Аналіз СЕМ-зображень зразків MP5 та MP10, синтезованих за однакової густини струму 0,50 А/см^2, але відповідно без ПАР та з вмістом 0,5 г/л ATLAS, показав істотну різницю у розмірах частинок. Частинки у зразку MP10 є в кілька разів дрібнішими порівняно зі зразком MP5, що свідчить про ефективну роль ATLAS як стабілізатора росту частинок і його здатність сприяти формуванню більш монодисперсного порошку.

Ключові слова: Електрохімічний синтез, Наночастинки, Цинк сульфід, Кристалографічна проєкція.